

A Unified Framework for Causal Estimand Selection

Martha Barnard*, Jared D. Huling, Julian Wolfson

Division of Biostatistics and Health Data Science, School of Public Health, University of Minnesota

Abstract

Estimating the causal effect of a treatment or health policy with observational data can be challenging due to an imbalance of and a lack of overlap between treated and control covariate distributions. In the presence of limited overlap, researchers choose between 1) methods (e.g., inverse probability weighting) that imply traditional estimands but whose estimators are at risk of considerable bias and variance; and 2) methods (e.g., overlap weighting) which imply a different estimand, thereby modifying the target population to reduce variance. We propose a framework for navigating the tradeoffs between variance and bias due to imbalance and lack of overlap and the targeting of the estimand of scientific interest. We introduce a bias decomposition that encapsulates bias due to 1) the statistical bias of the estimator; and 2) estimand mismatch, i.e., deviation from the population of interest. We propose two design-based metrics and an estimand selection procedure that help illustrate the tradeoffs between these sources of bias and variance of the resulting estimators. Our procedure allows analysts to incorporate their domain-specific preference for preservation of the original research population versus reduction of statistical bias. We demonstrate how to select an estimand based on these preferences with an application to right heart catheterization data.

Keywords: average treatment effect, causal inference, inverse probability weighting, propensity score, target population

* barna126@umn.edu

1 Introduction

A primary goal of healthcare research is to determine the causal effect of a treatment or policy on health outcomes. Estimating causal effects using observational data requires 1) an unconfounded comparison of treated and control groups such that the two groups have similar, or balanced, characteristics; and 2) overlap between the treated and control groups such that all observations have a non-zero probability of being assigned either treatment or control. While there are a wide variety of methods to adjust for covariate imbalance, overlap is less well-understood and there are relatively fewer methods that address its impacts on the estimation of causal effects. Some methods aim to reduce variance inflation caused by limited overlap through either achieving only approximate balance or by modifying the population of interest to a new population has sufficient overlap. Yet, these approaches, respectively, increase estimator bias or shift the target estimand away from the original estimand of scientific interest. It is also often unclear which method, or which estimand, is best suited for a given scientific question and degree of overlap. In this paper, we develop a framework for simultaneously navigating the tradeoffs between preserving the original target population and minimizing the bias and variance that can result from imbalance and lack of overlap.

1.1 Weighting methods for balancing covariates

There are many methods that balance the covariates between groups (e.g., regression, matching, weighting). We focus on weighting methods which reweight the data in order to achieve covariate balance. One set of such methods seek to directly balance the covariates by deriving weights subject to covariate constraints using optimization procedures (Hainmueller, 2012; Zubizarreta, 2015; Wang and Zubizarreta, 2020). Another set of methods rely on inverse probability weighting (IPW), where observations are inverse weighted by the sample probability of receiving their assigned treatment (Rosenbaum and Rubin, 1983a; Hahn, 1998; Robins et al., 2000; Hirano and Imbens, 2001; Hirano et al., 2003; Imbens, 2004). Both types of methods can target estimands corresponding to a specific population, such as the average treatment effect defined over the entire (ATE), treated (ATT), or control (ATC) sample population. While these methods target estimands with a meaningful population, a lack of overlap between the treated and control covariate distributions can create very large weights that produce estimators with inflated variance and the potential for considerable bias (Busso et al., 2014; Hong et al., 2020). While direct balancing methods generally provide more stable and smaller weights, a lack of overlap can yield no solutions to the optimization problem (Hainmueller, 2012; Chattopadhyay et al., 2020). Similar issues arise with matching methods, where large differences between the treated and control groups can result in bias in the treatment effect estimator due to imbalance.

1.2 Weighting methods that address lack of overlap

A variety of new weighting methods have been created that mitigate the impacts of lack of overlap on estimation. For the majority of these methods, reducing variance of the estimator is the primary goal. Wang and Zubizarreta (2020) explore a class of direct balancing weights called minimal weights which provide approximate, rather than exact balance of the covariate distributions, resulting in estimators with reduced variance but potentially increased bias. Other approaches work by modifying the estimand, and consequently the target population,

either explicitly or implicitly to achieve better overlap. Crump et al. (2009) formalize modifying the estimand through propensity score trimming while Li and Greene (2013) and Yang and Ding (2018) propose continuous weights that approximate pair matching and propensity score trimming, respectively. One of the more widely-used such methods is overlap weights (Li et al., 2018, 2019), which minimize the asymptotic variance of the weighted average treatment effect estimator across all estimands characterized by weighted populations under the assumption of homoscedasticity. Overlap weights emphasize individuals with propensity scores around 0.5, i.e. those with so-called clinical equipoise, targeting the “overlap” (ATO) population. Matching methods also often address lack of overlap by modifying the matched population and frequently operate by discarding hard-to-match samples, improving balance by modifying the population (Rosenbaum, 2012; de los Angeles Resa and Zubizarreta, 2016; Visconti and Zubizarreta, 2018).

There are a variety of scenarios in which it is reasonable to deviate from estimands that aggregate over the entire sample population; for example, some sample populations are a convenience sample (Rosenbaum, 2012) and as such, the ATE may not have clinical relevance. Li et al. (2018) and Mao et al. (2019) both argue that overlap weights target a population of interest; people with propensity scores around 0.5 may be the individuals for whom clinical treatment guidelines are unclear. While this is often true, in practice treatments and policies may not be assigned equitably along demographic factors (Faigle et al. (2017); Raeisi-Giglou et al. (2022); Tchikrizov et al. (2023)); in these cases, the interpretation of individuals at equipoise is unclear. Regardless of whether clinical equipoise is of interest, it can be hard to describe the exact population that is induced by overlap weights. Therefore, in many scenarios it is still desirable to estimate the ATE or ATT even in the presence of low overlap to preserve a meaningful and/or interpretable population. Among methods that address lack of overlap, there has been limited development on constructing an estimand that also has an interpretable population. Traskin and Small (2011) and Fogarty et al. (2016) propose methods for selecting an interpretable population with better overlap, though both methods can still produce estimators with considerable bias and/or variance.

1.3 Proposed framework

There are clear tradeoffs between retaining an estimand with a meaningful target population, estimator bias, and variance among current methods for treatment effect estimation when there is a lack of overlap. Standard weighting methods target estimands with meaningful populations, however there is risk of estimator bias and inflated variance. Methods such as minimal weights and overlap weights aim to minimize estimator variance, but in doing so they either sacrifice estimator bias or eschew the original target population. Most methods described above aim to improve or maintain only one of estimator bias, variance, or the target population, but the extent to which the other two characteristics are influenced for a given analysis is often unclear. Different biomedical or healthcare application may seek to prioritize these three characteristics differently; in some cases statistical performance may be the primary priority, while in others it may be important to maintain the population of interest. However, as far as we know, there are few or no methods that provide tools to flexibly explore and quantify the tradeoffs between all three characteristics.

In this work, we present a conceptual framework and corresponding procedure for charac-

terizing and selecting an estimand according to its target population, estimator bias, and variance, allowing the analyst to explicitly prioritize any of these properties. As part of the conceptual framework, we introduce a bias decomposition that encapsulates bias due to 1) the statistical bias of the estimator; and 2) estimand mismatch i.e., deviation from the population of interest. To leverage this decomposition for estimand selection, we propose two design-based metrics that target each part of the bias decomposition. Furthermore, we propose an estimand selection procedure that enumerates a sequence of estimands corresponding to different tradeoffs between preservation of the target estimand and statistical performance in terms of bias and variance, where the ATE, ATT, ATC, and ATO are special cases of the set of possible estimands under consideration. We analyze synthetic data from a variety of data generating scenarios and data from a right heart catheterization study to demonstrate the effectiveness of our method in navigating these tradeoffs. We present all methods and results in reference to the ATE as the estimand of scientific interest, however, all methods can apply to other estimands/populations such as the ATT.

The remainder of the paper is outlined as follows. In Section 2, we introduce notation and our conceptual framework for characterizing and selecting estimands. Section 3 describes the design-based metrics for characterizing both sources bias and the proposed estimand selection procedure. Section 4 validates our metrics and evaluates the performance of our estimation selection procedure in comparison to the ATE and ATO through simulation studies. In Section 5 we apply our entire procedure to reanalyze a study on right heart catheterization. Finally, Section 6 discusses the results and future work.

2 Conceptual framework for causal estimand selection

2.1 Notation and assumptions

Consider a sample $\{(Z_i, Y_i, \mathbf{X}_i)\}_{i=1}^n$ of size n from a population. For individual or unit i , let $Z_i = z$, indicate belonging to the treatment ($z = 1$) or control group ($z = 0$), Y_i be the outcome, and $\mathbf{X}_i = (X_{i1}, \dots, X_{ip})$ be a p length vector of covariates. Let $e(\mathbf{x}) = \Pr(Z_i = 1 | \mathbf{X}_i = \mathbf{x})$ be the propensity score. We use the potential outcomes framework (Neyman (1990); Rubin (1974, 1978); Hernan and Robins (2024)), where $Y(z)$ is the outcome that would be observed if assigned to treatment group z . In practice, only one potential outcome is observed per individual. We assume the standard stable unit treatment value assumption (SUTVA) that states the potential outcomes for each individual are unaffected by the treatment assignments of other individuals and that there is only one version of treatment, which implies that $Y_i = Y_i(Z_i)$. We also assume that the treatment effect is strongly unconfounded such that $\{Y(0), Y(1)\} \perp\!\!\!\perp Z | \mathbf{X}$, which requires that there are no unmeasured confounders. Finally, we assume positivity (Rosenbaum and Rubin (1983a)), which requires that $0 < e(\mathbf{x}) < 1$ such that all individuals have a non-zero probability of being assigned to either the treatment or control group. Given these assumptions and using potential outcomes notation, the conditional average treatment effect (CATE) is $\tau(\mathbf{x}) = \mu_1(\mathbf{x}) - \mu_0(\mathbf{x}) = E\{Y(1) - Y(0) | \mathbf{X} = \mathbf{x}\}$. Let $f(\mathbf{x})$ be the marginal distribution of the covariates and $h(\mathbf{x})$ some function such that $f(\mathbf{x})h(\mathbf{x})$ is the density of a target population. Then the estimand, τ_h , averages the CATE over the target population, $\tau_h = \frac{\int \tau(\mathbf{x})h(\mathbf{x})f(\mathbf{x})d\mathbf{x}}{\int h(\mathbf{x})f(\mathbf{x})d\mathbf{x}}$. Each $h(\mathbf{x})$ defines a different target population

and thus a different causal estimand. We assume that $\tau(\mathbf{x})$ varies with \mathbf{x} , such that averaging over different populations (i.e., different causal estimands) may yield different results. For a given weight function $h(\mathbf{x})$, Li et al. (2018) propose a class of propensity score balancing weights such that weighted covariate distributions are balanced between the two treatment groups,

$$w_1(\mathbf{x}) = \frac{h(\mathbf{x})}{e(\mathbf{x})} \text{ for } Z = 1, \text{ and } w_0(\mathbf{x}) = \frac{h(\mathbf{x})}{1 - e(\mathbf{x})} \text{ for } Z = 0. \quad (1)$$

For the ATE, which averages $\tau(\mathbf{x})$ over the entire covariate population, $h(\mathbf{x}) = 1$ and the balancing weights are the standard IPW weights. Other common causal estimands, such as the ATT or ATC, and their corresponding $h(\mathbf{x})$, weights, and target populations are in Supplementary Table 1. For a given $h(\mathbf{x})$, the sample estimator for τ_h is $\hat{\tau}_h = \frac{\sum_i w_1(\mathbf{X}_i) Z_i Y_i}{\sum_i w_1(\mathbf{X}_i) Z_i} - \frac{\sum_i w_0(\mathbf{X}_i) (1 - Z_i) Y_i}{\sum_i w_0(\mathbf{X}_i) (1 - Z_i)}$, where $\hat{\tau}_h$ is consistent for τ_h when the weights in Equation (1) are used (Li et al., 2018). For the following sections, aside from Section 2.4, we assume $\hat{\tau}_h$ is computed with estimated propensity scores as the true propensity scores are rarely known.

2.2 Decomposing sources of error in the presence of positivity violations

In practice, one may need to mitigate variability and/or bias due to lack of overlap by modifying the estimand from the original estimand. We call the modified estimand a “performance” estimand, as it is often chosen pragmatically. In this section, we aim to characterize the sources of discrepancy between the original target estimand of interest and the specific estimator used in practice, which may or may not target a performance estimand. This characterization allows us to systematically navigate the bias and variance tradeoffs that account for both statistical errors and mismatch between the original estimand and performance estimand.

We refer to the original estimand, which would typically correspond to a meaningful population and be viewed as the key estimand of scientific interest, as the population target estimand. Performance estimands, on the other hand, are often chosen to provide improved statistical benefits (e.g. lower estimator bias, variance) in comparison to the population target estimand. The population target and performance estimands can be the same; for example, the ATO provides variance reduction compared to other estimands and may also correspond to a population of interest. However, we will generally consider estimands such as the ATO and those induced by propensity score trimming as performance estimands as these estimands were originally proposed to achieve estimators with reduced variance. Throughout the rest of the paper, we will consider the ATE ($h(\mathbf{x}) = 1$), τ , as the population target estimand for demonstrative purposes, though the proposed methods and framing can straightforwardly apply to any target estimand.

Let $h_p(\mathbf{x})$ correspond to a performance estimand τ_{h_p} for a given analysis where the target estimand is τ . Then the bias of $\hat{\tau}_{h_p}$ in relation to τ can be decomposed as

$$E(\hat{\tau}_{h_p}) - \tau = \underbrace{E(\hat{\tau}_{h_p}) - \tau_{h_p}}_{\text{Statistical bias}} + \underbrace{\tau_{h_p} - \tau}_{\text{Estimand mismatch}}. \quad (2)$$

The first term represents the statistical bias of the estimator $\hat{\tau}_{h_p}$, while the second term represents the mismatch between the ATE and the performance estimand. To minimize the discrepancy between $\hat{\tau}_{h_p}$ and the target estimand, both the estimand mismatch and the statistical bias of $\hat{\tau}_{h_p}$ must be controlled. Estimand mismatch and statistical bias are often at odds, especially in scenarios with substantial positivity violation; for example, $\tau_{h_p} = \tau$ would yield zero estimand mismatch, but $\hat{\tau}$ tends to have high statistical bias when there is low overlap. To reduce overall bias, it is desirable to identify a τ_{h_p} such that $\hat{\tau}_{h_p}$ has smaller statistical bias than $\hat{\tau}$ as well as limited estimand mismatch.

To help navigate the tradeoffs between estimand mismatch, statistical bias, and variance we propose an approach for the selection of the performance estimand, τ_{h_p} . We allow for selection of τ_{h_p} from the following family of potential weight functions,

$$h_{c,d}(\mathbf{x}) = e(\mathbf{x})^c \{1 - e(\mathbf{x})\}^d; 0 \leq c, d \leq 1, \quad (3)$$

where the ATE, ATC, ATT, and ATO are all special cases of this set (Figure 1). By varying the two parameters, c and d , this family provides a smooth transition between each of these widely-used estimands. We can then select τ_{h_p} from this set by characterizing the bias and variance of their corresponding estimators.

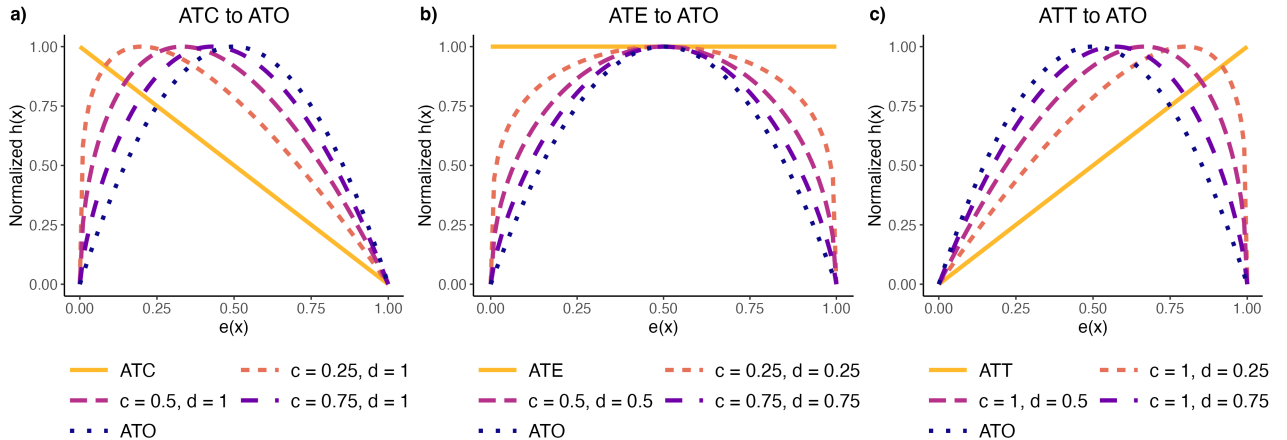


Figure 1: We show the normalized $h(\mathbf{x})$ in relation to the propensity score, $e(\mathbf{x})$, for a set of estimands. For each subplot, we plot $h(\mathbf{x})$ for a well-known estimand and the ATO and demonstrate how estimands within our proposed set (Equation (3)) are intermediaries between them.

2.3 Identifying measurable attributes of estimand mismatch and statistical bias

To leverage the bias decomposition proposed in the previous section for estimand selection, it is necessary to understand the measurable attributes that impact estimand mismatch and statistical bias. We focus on the ATE as the target estimand, however, this work can also be applied to other estimands of interest such as the ATT, ATC, or when transporting the effect to a new population. For clarity in notation, we assume that the weights have been normalized such that $\sum_{i=1}^n w_z(\mathbf{X}_i)I(Z_i = z) = n_z$, the sample size of treatment group z . We

can then express the difference between a performance estimator and the ATE as

$$\hat{\tau}_{h_p} - \tau = \underbrace{\int \mu_1(\mathbf{x}) d\{F_{n_0,0,w_0} - F_n\}(\mathbf{x}) - \int \mu_0(\mathbf{x}) d\{F_{n_1,1,w_1} - F_n\}(\mathbf{x})}_{\text{Estimand mismatch}} \quad (4)$$

$$+ \underbrace{\int \{\mu_1(\mathbf{x}) + \mu_0(\mathbf{x})\} d\{F_{n_1,1,w_1} - F_{n_0,0,w_0}\}(\mathbf{x})}_{\text{Statistical bias}} \quad (5)$$

$$- \int \{\mu_1(\mathbf{x}) - \mu_0(\mathbf{x})\} d\{F - F_n\}(\mathbf{x}) \quad (6)$$

$$+ \frac{1}{n_1} \sum_{i=1}^n w_1(\mathbf{X}_i) \epsilon_i Z_i - \frac{1}{n_0} \sum_{i=1}^n w_0(\mathbf{X}_i) \epsilon_i (1 - Z_i), \quad (7)$$

where $\epsilon_i = Y_i(Z_i) - \mu_{Z_i}(\mathbf{X}_i)$, $F_n(\mathbf{x}) = \sum_{i=1}^n I(\mathbf{X}_i \leq \mathbf{x})/n$ is the empirical CDF, and $F_{n_z,z,w_z}(\mathbf{x}) = \sum_{i=1}^n w_z(\mathbf{X}_i) I(\mathbf{X}_i \leq \mathbf{x}, Z_i = z)/n_z$ is the weighted empirical CDF. In this expression, term (6) goes to zero for a representative sample of the population and term (7) has mean zero. Then, the difference between our performance estimator and population target estimand can be characterized by terms (4) and (5) which are induced by estimand mismatch and statistical bias, respectively. We note that term (4) often has non-zero expectation even with no estimand mismatch (the expectation is zero when using the true propensity scores); however, this term does tend to increase in size as estimand mismatch increases. The measurable quantities in terms (4) and (5) are 1) the imbalance between the empirical CDFs F_n and F_{n_z,z,w_z} ; and 2) the imbalance between empirical CDFs $F_{n_0,0,w_0}$ and $F_{n_1,1,w_1}$. To formally characterize estimand mismatch and statistical bias for a given $\hat{\tau}_{h_p}$, we propose design-based metrics that measure these two distributional imbalances in Sections 3.1 and 3.2. To select a performance estimand from the family of $h(\mathbf{x})$ in Equation (3), we evaluate $h_{c,d}(\mathbf{x})$ by these two metrics.

2.4 Identifying estimands with minimal estimator variance

While we have focused on estimator bias, we also often want to identify a performance estimand whose corresponding estimator has small or minimal variance. Li et al. (2018) prove that overlap weights ($h(\mathbf{x}) = e(\mathbf{x})\{1 - e(\mathbf{x})\}$) yield the estimator with the minimum asymptotic variance for all $\hat{\tau}_h$ under homoscedasticity. However, overlap weights do not necessarily yield the estimator with minimum asymptotic variance when homoscedasticity does not hold. The following proposition establishes the variance conditions under which $\hat{\tau}_{h^*}$ has minimum asymptotic variance (proof in Appendix A).

Proposition 1. *Let $v_z(\mathbf{x}) = \text{Var}\{Y(z)|\mathbf{X} = \mathbf{x}\}$ and $h^*(\mathbf{x}) > 0$ for all \mathbf{x} . Then if*

$$v_0(\mathbf{x}) = v \frac{k_0(\mathbf{x})\{1 - e(\mathbf{x})\}}{h^*(\mathbf{x})\{k_0(\mathbf{x}) + k_1(\mathbf{x})\}} \text{ and } v_1(\mathbf{x}) = v \frac{k_1(\mathbf{x})e(\mathbf{x})}{h^*(\mathbf{x})\{k_0(\mathbf{x}) + k_1(\mathbf{x})\}},$$

$h(\mathbf{x}) \propto h^(\mathbf{x})$ gives the minimum asymptotic variance of all balancing weight estimators $\hat{\tau}_h$ for $v \in \mathbb{R}^+$ and functions $k_0(\mathbf{x}), k_1(\mathbf{x}) > 0$ for all \mathbf{x} .*

This result further motivates selecting a performance estimand specific to a given dataset, as the overlap weights estimator $\hat{\tau}_h$ may not have the minimum asymptotic variance let alone the

minimum finite sample variance for some data. To characterize estimator variance and select a performance estimand, we estimate the standard error of each $\hat{\tau}_{h_{c,d}}$ using a bootstrapped standard error estimator (Crump et al., 2009).

3 Implementation of estimand selection framework

3.1 Characterizing estimand mismatch

We use the weighted energy distance as our measure of imbalance between distributions (Huling and Mak, 2024). We choose the energy distance due to its performance in high dimensions and computational efficiency, however other measures of distributional imbalance such as the maximum mean discrepancy, Wasserstein distance, etc. could work well and be used here instead. The weighted energy distance between empirical CDFs F_n and F_{n_z, z, w_z} is

$$\begin{aligned} \mathcal{E}(F_{n_z, z, w_z}, F_n) &= \frac{2}{n_z n} \sum_{i=1}^n \sum_{j=1}^n w_z(\mathbf{X}_i) I(Z_i = z) \|\mathbf{X}_i - \mathbf{X}_j\|_2 - \frac{1}{n^2} \sum_{i=1}^n \sum_{j=1}^n \|\mathbf{X}_i - \mathbf{X}_j\|_2 \\ &\quad - \frac{1}{n_z^2} \sum_{i=1}^n \sum_{j=1}^n w_z(\mathbf{X}_i) w_z(\mathbf{X}_j) I(Z_i = Z_j = z) \|\mathbf{X}_i - \mathbf{X}_j\|_2. \end{aligned}$$

In this context, $\mathcal{E}(F_{n_z, z, w_z}, F_n)$ quantifies the difference between the population that is generated by $h_{c,d}(\mathbf{x})$ and the target ATE population. While non-zero energy distances indicate the degree of difference between two distributions, the energy distance is not a standardized metric and therefore is not comparable across different weight functions. To create a metric comparable across all $h_{c,d}(\mathbf{x})$, we construct a permutation-based statistical test for $H_0 : F = F_{z, w_z}$. The proposed test procedure for a given F_n and F_{n_z, z, w_z} follows:

1. Compute the test statistic $\mathcal{E}(F_{n_z, z, w_z}, F_n)$
2. For $b = 1, \dots, B$: i) Sample $F_{n_z}^{(b)}$ from F_n without replacement; ii) Compute $\mathcal{E}(F_{n_z, w_z}^{(b)}, F_n)$
3. Compute the p -value, $p = \frac{1}{B} \sum_{b=1}^B I[\mathcal{E}(F_{n_z, z, w_z}, F_n) \leq \mathcal{E}(F_{n_z, w_z}^{(b)}, F_n)]$

In step 2, since w_z has no relationship to the randomly sampled $\{F_{n_z}^{(b)}\}_{b=1}^B$, $\{F_{n_z, w_z}^{(b)}\}_{b=1}^B$ approximates F_{z, w_z} under the desired null $F = F_{z, w_z}$. We can use this p -value for inference or simply as a standardized measure of the imbalance between F_{n_z, z, w_z} and F_n , where smaller p -values tend to correspond to $\hat{\tau}_{h_{c,d}}$ with higher potential for large estimand mismatch. If we want to determine whether the population induced by $h_{c,d}(\mathbf{x})$ is different from the ATE population, we reject the null hypothesis that these populations are the same at $p < \alpha = 0.05$. In Sections 4 and 5, we use the minimum of the p -values computed for each treatment group z as the main design-based metric for characterizing estimand mismatch.

3.2 Characterizing statistical bias

Let G indicate the CDF for the fitted propensity scores $\hat{e}(\mathbf{X}_i)$. The weighted energy distance between empirical CDFs $G_{n_0,0,w_0}$ and $G_{n_1,1,w_1}$ is

$$\begin{aligned} \mathcal{E}(G_{n_0,0,w_0}, G_{n_1,1,w_1}) &= \frac{2}{n_0 n_1} \sum_{i=1}^n \sum_{j=1}^n w_0(\mathbf{X}_i) w_1(\mathbf{X}_j) I(Z_i = 0) I(Z_j = 1) \|\hat{e}(\mathbf{X}_i) - \hat{e}(\mathbf{X}_j)\|_2 \\ &\quad - \sum_{z=0}^1 \frac{1}{n_z^2} \sum_{i=1}^n \sum_{j=1}^n w_z(\mathbf{X}_i) w_z(\mathbf{X}_j) I(Z_i = Z_j = z) \|\hat{e}(\mathbf{X}_i) - \hat{e}(\mathbf{X}_j)\|_2. \end{aligned}$$

We use the propensity score empirical CDFs instead of the covariate empirical CDFs (as seen in term (5)) because the use of propensities scores has been shown to be sufficient for covariate sample balance (Rosenbaum and Rubin, 1983b) and to simplify computation. The permutation-based statistical test procedure for $H_0 : G_{0,w_0} = G_{1,w_1}$ follows:

1. Compute $\mathcal{E}(G_{n_0,0,w_0}, G_{n_1,1,w_1})$
2. For $b = 1, \dots, B$: i) Permute the treatment assignments to generate $G_{n_0}^{(b)}$ and $G_{n_1}^{(b)}$; ii) Compute $\mathcal{E}(G_{n_0}^{(b)}, G_{n_1}^{(b)})$
3. $p = \frac{1}{B} \sum_{b=1}^B I[\mathcal{E}(G_{n_0,0,w_0}, G_{n_1,1,w_1}) \leq \mathcal{E}(G_{n_0}^{(b)}, G_{n_1}^{(b)})]$

In step 2, permuting the treatment assignment breaks the relationship between treatment assignment and covariates such that $\{G_{n_0}^{(b)}, G_{n_1}^{(b)}\}_{b=1}^B$ approximate G_0, G_1 under $G_0 = G_1$ which is equivalent to the desired null $G_{0,w_0} = G_{1,w_1}$ in population. Here, we primarily use p as a standardized measure of the imbalance between $G_{n_0,0,w_0}$ and $G_{n_1,1,w_1}$, where smaller p -values tend to correspond to $\hat{\tau}_{h_{c,d}}$ with the potential for larger statistical bias. We are less interested in specifying an α level as $\mathbf{w}_0, \mathbf{w}_1$ are designed to make these distributions equal and thus we expect these p -values to generally be high. While this p -value is motivated by characterizing statistical bias due to lack of overlap, in practice it characterizes statistical bias due to any source(s), such as propensity model misspecification.

3.3 Estimand selection

We propose the following selection procedure as an approach for enumerating a sequence of estimators, each approximately optimal (i.e., low potential for statistical bias and low estimator variance) for a given subjective choice in emphasis of estimand mismatch versus statistical bias. Thus, the procedure allows the analyst to choose the point along this spectrum most appropriate for their research question. The procedure is as follows:

1. Compute p as defined in Sections 3.1 and 3.2 and the bootstrapped standard error estimator for some grid of potential $h_{c,d}(\mathbf{x})$, $c, d \in [0, 1]$.
2. For each set of p -values, (i.e., corresponding to estimand mismatch and statistical bias) create density contours on the $(c, d) \in [0, 1] \times [0, 1]$ space (Supplementary Figure 1a) and use kriging to interpolate the estimated standard errors across a finer grid.

3. Intersect the estimand mismatch and statistical bias p -value contours. For each estimand mismatch p -value contour level, identify the area intersecting with the largest statistical bias p -value contour level and select the $h_{c,d}(\mathbf{x})$ with the smallest estimated standard error in that area (Supplementary Figure 1b)).

The first step in the procedure characterizes a grid of estimands by the proposed estimand mismatch and statistical bias metrics as well as estimated standard error. The second step simply extends this characterization across either all estimands defined by Equation (3) or a finer grid of estimands. Step three identifies and selects an estimand with low potential for statistical bias and the smallest estimated standard error within each estimand mismatch p -value contour. This results in a sequence of estimands; as the estimand mismatch p -value contour level gets smaller, the selected estimand tends to have larger estimand mismatch but smaller estimator statistical bias and variance.

In general, we recommend selecting the estimand identified within the $(0.05, 0.1]$ p -value contour, as the corresponding estimator will tend to have the lowest standard error among estimands where we fail to reject the null hypothesis that the weighted estimand population is the same as the ATE population. Although we propose this procedure and implement it within Sections 4 and 5, it can be varied depending on the particular data application. For example, if only the statistical performance of the estimator is of interest, one could select the estimand in the largest statistical bias p -value contour with the smallest estimated standard error. Ultimately, the selection procedure can be adapted based on the perceived importance of estimand mismatch, statistical bias, and estimator variance in a given application.

4 Simulation experiments

4.1 Methods

We construct data generating scenarios with varying levels of propensity score overlap, treatment effect heterogeneity, and percent of treated individuals. Through these scenarios, we aim to validate the metrics proposed in Sections 3.1 and 3.2 across a variety of data generating processes. In addition, we aim to illustrate the scenarios in which our estimand selection procedure can identify estimands whose corresponding estimators have benefits over the ATE and ATO estimators. We also demonstrate how the different data generation attributes influence the bias-variance tradeoffs of estimand selection within our procedure.

4.1.1 Data generation and characterizing estimands

We implement nearly the same simulation data generation process as in Li et al. (2019). Here, we drop the observation index on variables for clarity of presentation. We generate V_1, \dots, V_6 from a multivariate normal distribution with $E[V_i] = 0$, $Var(V_i) = 1$ for all $i = 1, \dots, 6$ and $Cov(V_i, V_j) = 0.5$ for all $i \neq j$. We take $X_1 - X_3 = V_1 - V_3$ and dichotomize $V_4 - V_6$ such that $X_j = I[V_j < 0]$ for $j = 4, 5, 6$. The true propensity scores are generated as $e(\mathbf{X}) = \{1 + \exp(-\alpha_0 - \sum_{j=1}^6 \alpha_j X_j)\}^{-1}$. Our continuous outcome, Y , is generated as $Y \sim N\{E(Y|Z, \mathbf{X}), 1\}$ where $E(Y|Z, \mathbf{X}) = \beta_0 + \sum_{j=1}^6 \beta_j X_j + \Delta(\mathbf{X})Z$. Similar to Mao et al. (2019), we choose two treatment effect functions that have a concave relationship with $e(\mathbf{X})$. The two functions have different ranges that represent the level of treatment effect heterogeneity, 1) Medium: $\Delta(\mathbf{x}) = 8e(\mathbf{x})\{1 - e(\mathbf{x})\}$ and 2) High: $\Delta(\mathbf{x}) = 16e(\mathbf{x})\{1 - e(\mathbf{x})\} - 1$. Consistent with

Li et al. (2019), the parameters for the true propensity score model are $(\alpha_1, \alpha_2, \alpha_3, \alpha_4, \alpha_5, \alpha_6) = (0.15\gamma, 0.3\gamma, 0.3\gamma, -0.2\gamma, -0.25\gamma, -0.25\gamma)$ and α_0 is chosen to generate the desired percent of treated individuals (25% and 50%). We explore $\gamma = 1, 2, 3, 4$ where $\gamma = 1$ generates data with substantial propensity score overlap and $\gamma = 4$ generates data with minimal propensity score overlap and substantial density of propensity scores in the tails (Supplementary Figure 2). For our outcome model, we set $(\beta_0, \beta_1, \beta_2, \beta_3, \beta_4, \beta_5, \beta_6) = (0, -0.5, -0.5, -1.5, 0.8, 0.8, 1)$.

We have a total of 16 simulation scenarios that represent all combinations of $\gamma = 1, 2, 3, 4$, 25% and 50% treated individuals, and medium and high treatment effect heterogeneity. For each simulation scenario we generate 1000 independent datasets with 1000 observations each. For each simulated dataset, we use all combinations of $c, d = 0, 0.05, 0.1, \dots, 1$ as the grid of candidate estimand values (441 estimands). We calculate the true value of each estimand using 10 million Monte Carlo samples. For each estimand, we calculate the average treatment effect estimate, absolute percent statistical bias, and the average p -values from the two proposed metrics (Sections 3.1 and 3.2).

4.1.2 Estimand selection

Using the results from 4.1.1, we select a sequence of estimands for each simulated dataset with our proposed estimand selection procedure (Section 3.3). We use cubic spline interpolation to smooth the p -value contours and interpolate standard error estimates over a 500×500 grid using kriging with a Gaussian variogram model. With our procedure, the number of selected estimands varies by the range of estimand mismatch p -values in the data; thus, for each estimand mismatch p -value contour level, only a subset of the 1000 datasets have a corresponding selected estimand. Since the set of datasets that have a specific range of estimand mismatch p -values may differ systematically, we select two different sample size cutoffs ($n = 500, 900$) to compute aggregate metrics over. We calculate the MSE with respect to the true ATE for the ATE estimator, the estimators corresponding to estimands selected with our method, and the ATO estimator.

4.2 Results

4.2.1 Characterizing estimand mismatch

For the 50% treated scenarios, the estimands with $p > 0.05$ (i.e., the estimands whose weighted covariate populations are similar to the ATE covariate population) follow the region along the diagonal ($c = d$) which, at high propensity score overlap, goes between the ATE to the ATO (Figure 2, left panel). For all of these estimands, $h_{c,d}(\mathbf{x})$ peaks around propensity scores of 0.5. In contrast, for the 25% treated scenarios, the estimands with $p > 0.05$ follow a trend above the diagonal ($c < d$) such that $h_{c,d}(\mathbf{x})$ peaks at propensity scores around 0.25. Therefore, estimands that induce a covariate population similar to the ATE population are estimands where $h_{c,d}(\mathbf{x})$ peaks at the proportion of treated individuals. As propensity score overlap decreases, fewer estimands yield $p > 0.05$ and these estimands tend to have c, d close to the ATE (e.g. $c, d < 0.25$).

For the 25% treated scenarios, there is a clear relationship between the p -value metric and absolute estimand mismatch; estimand mismatch tends to be smallest along a trend above the diagonal (Figure 2, right panel). However, for the 50% treated scenarios, this relationship is not as immediately clear. Estimand mismatch depends not only on distributional imbalance,

but also on how the treatment effect varies across the covariate distribution (see term (4)). Therefore, $p < 0.05$ from our proposed metric indicates estimands with the *potential* for large absolute estimand mismatch, but the exact relationship will vary by data generating mechanism. When data is generated with a treatment effect that is a linear function of $e(\mathbf{X})$, there is clearer visual relationship between the p -value metric and estimand mismatch for the 50% treated scenarios; the estimands with the smallest estimand mismatch follow the diagonal (Supplementary Figure 3).

For all 25% treated data generating scenarios, no estimands with absolute estimand mismatch above the 0.20 quantile have $p > 0.05$. For 50% treated scenarios, no estimands with an absolute estimand mismatch above the 0.45 quantile have $p > 0.05$, except for the $\gamma = 1, 2$ scenarios from Figure 2. However, in these scenarios the absolute estimand mismatch is relatively small and therefore selecting any of the proposed estimands will yield low estimand mismatch. Thus, the p -value metric protects against selecting estimands with high estimand mismatch across a variety of data generating mechanisms.

4.2.2 Characterizing statistical bias

For both proportion treated scenarios, the p -values characterizing statistical bias tend to be largest at $c, d > 0.75$, close to the ATO (Figure 3, left panel). As propensity score overlap decreases the p -values get smaller, indicating that the estimators have a higher potential for statistical bias. For the 50% treated scenarios, the region of higher p -values tends to move from the ATO to the ATE along the diagonal. For the 25% treated scenarios, estimands above the diagonal ($c < d$) tend to have lower p -values (and therefore a higher potential for statistical bias) relative to the 50% treated scenario.

There is a strong relationship between the p -values and absolute percent statistical bias, as measured by Spearman’s correlation coefficient (Figure 3, right panel). The correlation tends to increase as propensity score overlap decreases; thus, as the potential for statistical bias gets higher, the p -value metric has a stronger relationship with statistical bias. Only in one scenario (50% treated, $\gamma = 1$) is there a weak relationship between the p -value and absolute percent statistical bias, however, all the estimands in this scenario have small statistical bias ($< 0.5\%$ bias). We find that estimands with $p < 0.30$ are at risk of substantial bias, with at least 28.6% of corresponding estimators having absolute percent statistical bias greater than 5%. While the exact numerical relationship between the p -value and absolute percent statistical bias will differ by data generating scenario, statistical bias tends to increase considerably as p gets close to zero (Supplementary Figure 4).

4.2.3 Estimand selection

Across data generating scenarios (for a $n = 500$ cutoff), the estimators corresponding to estimands selected with our method have a lower mean squared error (MSE) with respect to the ATE than either the ATE or ATO estimators (Figure 4). The curves in Figure 4, specifically within low-medium propensity score overlap ($\gamma = 3$) scenarios, help demonstrate the bias-variance tradeoff when the scientific interest is with respect to the ATE. For medium Δ heterogeneity, both the ATE (tends to have large variance) and ATO (tends to have substantial bias due to estimand mismatch) estimators have a large MSE indicating that bias and variance contribute relatively equally to the MSE. Thus, the estimators selected

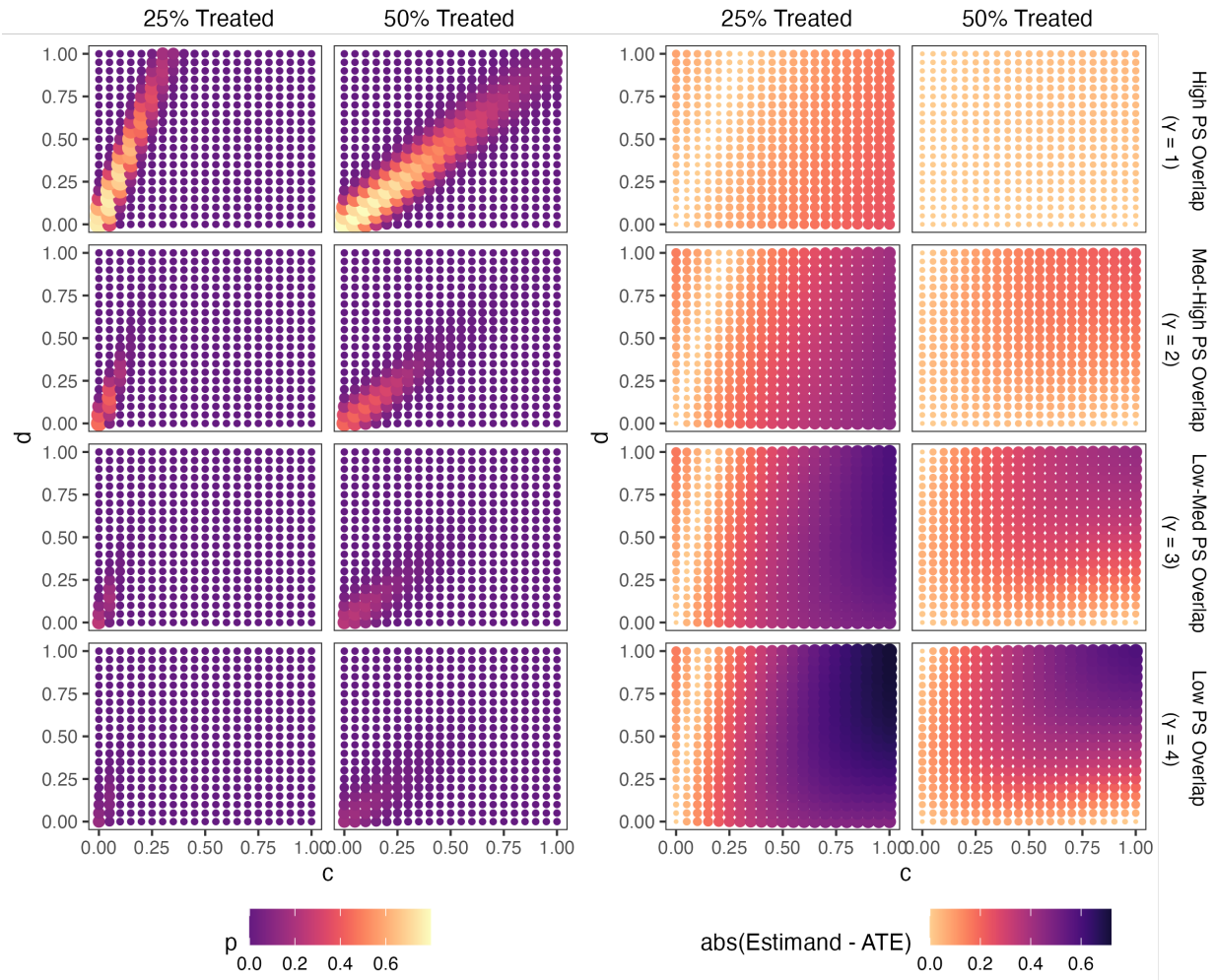


Figure 2: The left panel presents the average of the minimum of the two estimand mismatch related p -values, calculated as described in Section 3.1, for each estimand. The right panel presents the absolute difference between the true estimands and the true ATE (i.e., the absolute estimand mismatch) under the medium Δ heterogeneity scenario. Columns distinguish the 25% and 50% treated scenarios while rows distinguish the different propensity score overlap scenarios.

by our method all have lower MSE than the ATE and ATO estimators by moderating the size of both bias and variance. In contrast, for high Δ heterogeneity, the ATO estimator has a much larger MSE than the ATE estimator, indicating that bias (specifically estimand mismatch) dominates the MSE. Thus, estimators corresponding to larger estimand mismatch p -value contour levels tend to have the smallest MSE as they have reduced statistical bias and variance compared to the ATE estimator without incurring substantial estimand mismatch. We identify similar trends with a sample size cutoff of $n = 900$ (Supplementary Figure 5). The average estimand per estimand mismatch p -value contour level, across all datasets, is shown in Supplementary Figure 6. Consequently, there is a clear intuition for selecting a single estimand from the sequence of estimands identified through our method. If treatment effect heterogeneity is expected to be low, the estimands from smaller p -value contours will

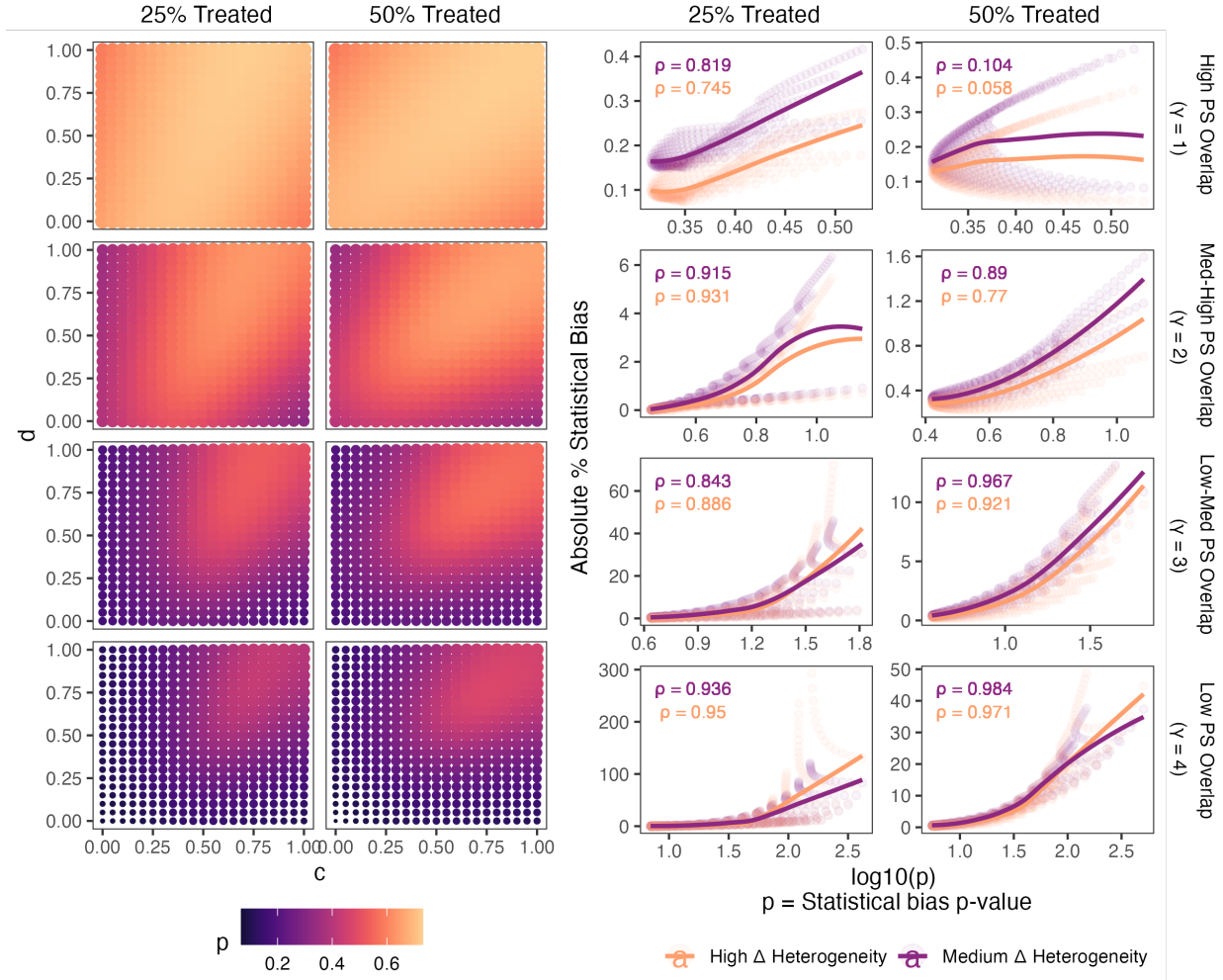


Figure 3: The left panel presents the average p -value corresponding to the statistical bias metric, calculated as described in Section 3.2, for each estimand. The right panel presents the relationship and Spearman correlation coefficient (ρ) between $\log_{10}(p)$ and the absolute percent statistical bias of the estimator for each estimand. Columns distinguish the 25% and 50% treated scenarios while rows distinguish the different propensity score overlap scenarios.

tend to minimize the MSE; if treatment effect heterogeneity is expected to be high, the estimands from larger p -value contours will tend to minimize the MSE. For applications where variance reduction has higher priority than retaining the target estimand, either the ATO or the estimands from the smallest p -value contours will tend to be superior estimand choices. For applications where bias reduction with respect to the target estimand is the priority, estimands from larger p -value contours will tend to perform the best. In general, estimands selected from our method tend to have lower MSE than either the ATE or ATO because they are intermediate options within the bias-variance tradeoff; they tend to mitigate the size of statistical bias, estimand mismatch, and variance rather than minimizing just one of these attributes.

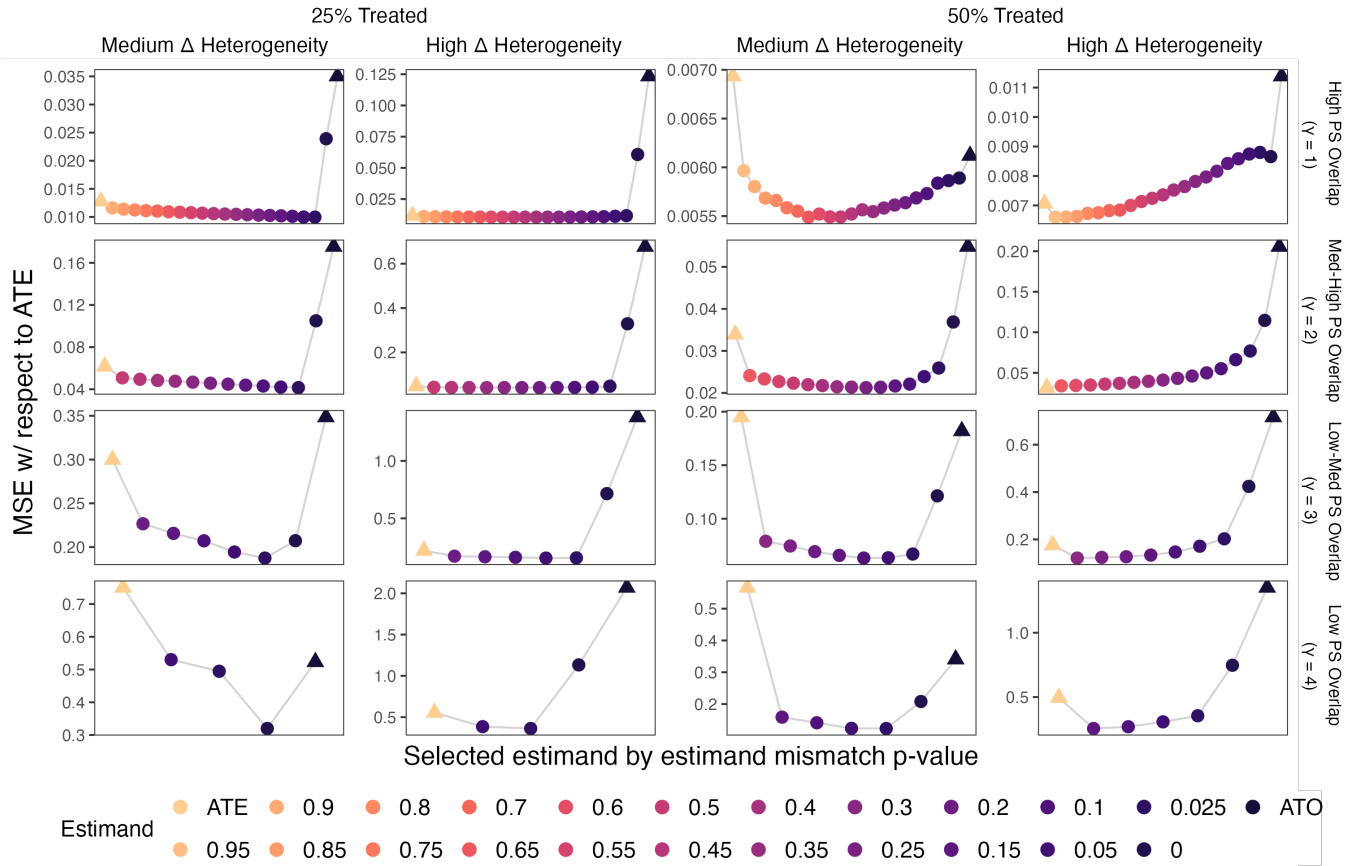


Figure 4: Mean squared error (MSE) with respect to the true ATE for the estimators for the ATE, the estimands selected with our procedure, and the ATO. Each of the 16 subplots corresponds to a single simulation scenario as labeled by the top and right axes. Estimands selected from our framework are labeled by the lower bound of their corresponding estimand mismatch p -value contour. From left to right in each subplot, the depicted estimands become less similar the ATE and more similar to the ATO. Estimands selected (i.e., estimand mismatch p -value contours present) in at least 500 of the simulated datasets are shown.

5 Application to right heart catheterization data

Right heart catheterization (RHC) is an invasive medical procedure that is performed on critically ill patients in order to measure cardiac function. An observational study by Connors et al. (1996) examined the impact of RHC on survival for patients in the ICU. The study was conducted between 1989-1994 across five medical centers within the United States. To account for treatment selection bias within the data, the authors matched treated and untreated individuals by propensity score matching as part of their analysis (Rosenbaum and Rubin (1983a,b)). The data has also been re-analyzed in various other works (Hirano and Imbens, 2001; Crump et al., 2009; Rosenbaum, 2012; Li et al., 2018; Huling and Mak, 2024). The primary analysis showed that RHC may be detrimental to survival, which was contrary to the popular belief that RHC improved patient outcomes.

The data consists of 5735 individuals, with 2184 treated (RHC applied within 24 hours of

hospital admission) and 3551 controls. The outcome of interest is an indicator of survival at 30 days and there are 71 covariates selected by a panel of experts as variables that relate to practitioners’ decision about whether to use RHC (Connors et al. (1996)). We estimate the propensity score using a logistic regression with all covariates and age squared, as both younger and older patients are less likely to receive RHC. There is low to moderate overlap in the estimated propensity scores of the treated and control groups and many propensity scores are close to zero (Supplementary Figure 7). This indicates that there is potential for poor statistical performance of the ATE estimator. When applying IPW weights, the average absolute standardized mean difference (SMD) of treated and control covariates after weighting is 0.018 and the maximum is 0.062; in general, the treated and control groups are relatively balanced after weighting (Supplementary Figure 8). For illustrative purposes, we quantitatively assess treatment effect heterogeneity through a series of linear probability models and find minimal evidence that there is substantial treatment effect heterogeneity within the data. In practice, this assessment would impact downstream inference. We apply our methods as described in Section 3 to characterize and select a sequence of estimands. We use a grid of all combinations $c, d = 0, 0.05, 0.10, \dots, 1$ and 1,000 null distribution or bootstrap replications for all metrics.

For the p -values pertaining to estimand mismatch, the estimands with $p > 0.05$ generally follow a linear trend above the diagonal on the plot; for these estimands, $h(\mathbf{x})$ peaks around propensity scores of 0.38, the proportion of treated individuals in the data (Figure 5). The p -values for characterizing statistical bias are largest for the estimands in the top right corner of the plot around the ATO. Of note, the statistical bias p -values are quite small (between 0 and 0.40); only only estimands with $c, d \geq 0.8$ have p -values greater than 0.30. This indicates that the estimators for many of the estimands have a high potential for statistical bias. In comparison to simulations, here we do not know the true propensity score model, and therefore the p -values characterize the potential for statistical bias both from the lack of overlap and any propensity model misspecification.

There are multiple ways to select a single estimand based on the tradeoffs between the three metrics. First, we reiterate that these estimands only differ when there is treatment effect heterogeneity. Therefore, in cases with minimal treatment effect heterogeneity, estimand mismatch may be a lower priority than statistical bias regardless of whether the ATE population is of interest. For this data, there is moderate to low evidence of treatment effect heterogeneity, which indicates we may want to prioritize minimizing estimator bias and standard error rather than estimand mismatch. When focusing only on these two metrics, the $p = 0$ estimand is the preferred estimand as it is in the largest statistical bias p -value contour and its estimator has the lowest estimated standard error (Figure 6). If we want to maximize the performance of our selected estimand while targeting a population similar to the ATE population, we could choose either the $p = 0.05$ or $p = 0.10$ estimand as they, respectively, are in the highest statistical bias p -value contour or have the lowest estimated standard error of all estimands with estimand mismatch $p > 0.05$. If there is belief in or evidence of substantial treatment effect heterogeneity, we would potentially want to select an estimand with likely smaller estimand mismatch, such as the $p = 0.20$ estimand. For this analysis, any of the $p = 0$, $p = 0.05$, or $p = 0.10$ estimands may be ideal due to the limited treatment effect heterogeneity exhibited in the data.

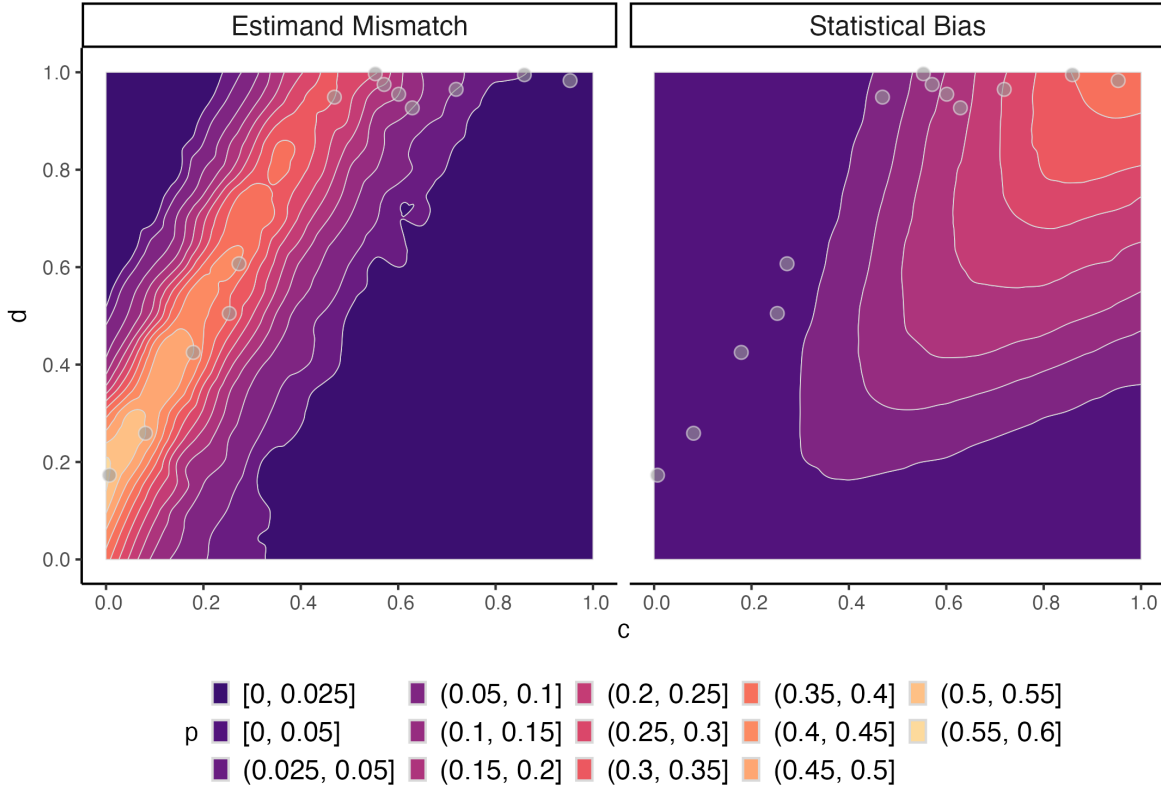


Figure 5: Contours of the p -values corresponding to estimand mismatch and statistical bias for the right heart catheterization study. Points on the figures show the estimands selected by our method (Section 3.3) for each estimand mismatch p -value contour. Note that the estimand mismatch panel has contours of $[0, 0.025]$ and $(0.025, 0.05]$ while the statistical bias panel only has the contour $[0, 0.05]$.

For illustrative purposes, we examine the treatment effect estimates of the selected estimands (Figure 6). The treatment effect estimate is around -0.056 for the ATE estimator and tends to decrease as the estimands become more similar to the ATO, whose estimate is around -0.065 ; all estimates indicate a negative effect of RHC on 30 day survival. The ATO and all estimands from estimand mismatch contours with $p < 0.35$ have similar treatment effect estimates around -0.065 . A re-analysis of this data by Hirano and Imbens (2001) using regression augmented estimators, which are more robust to model misspecification, found that when using propensity score and regression models with at least 15 covariates, the treatment effect estimates ranged from -0.059 to -0.067 . Since these results are similar to treatment effect estimates from the ATO and similar selected estimands, there is evidence that these estimands may yield estimates closer to the true ATE than the ATE estimator due to a reduction statistical bias while not incurring substantial estimand mismatch.

6 Discussion

Covariate imbalance and a lack of overlap pose significant challenges when estimating a causal treatment effect in a target population. To address these challenges, we have introduced a

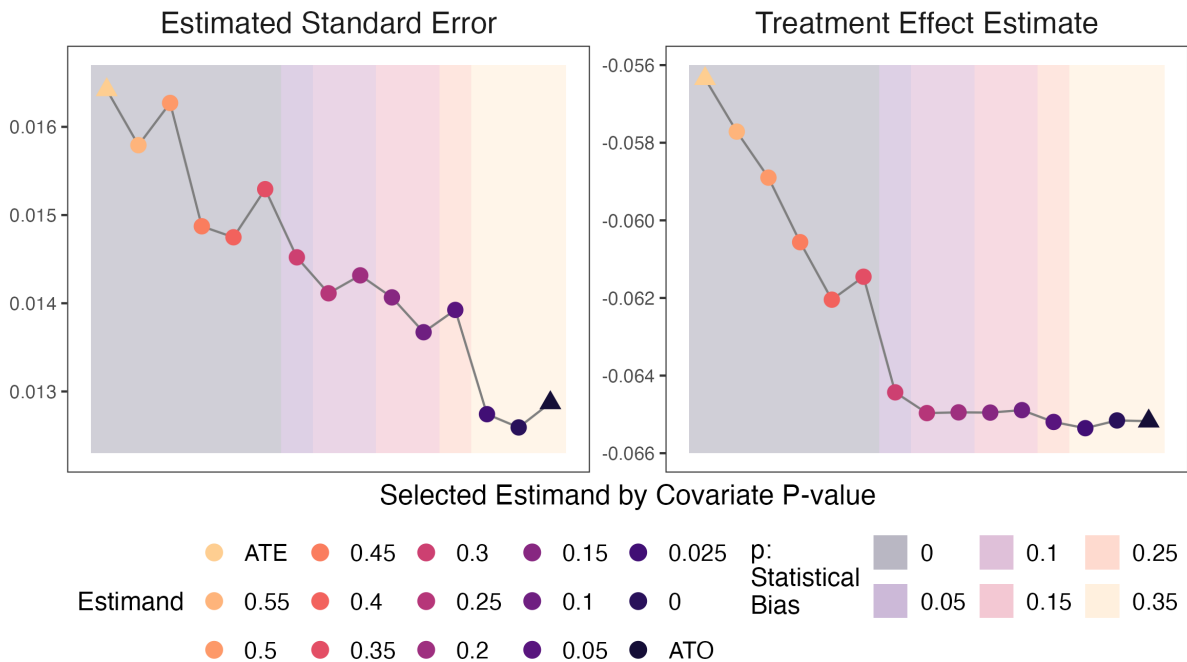


Figure 6: Characteristics of the ATE, selected estimands, and ATO for the right heart catheterization study. The selected estimands are labeled by the lower bound of their corresponding estimand mismatch p -value contour. Generally, lighter colors indicate estimands with better performance with respect to one aspect of the bias decomposition; lighter points indicate smaller potential for estimand mismatch, while lighter background shading indicates smaller potential for statistical bias.

framework for characterizing and selecting causal estimands based on the population targeted and the corresponding estimator’s statistical bias and variance. We have proposed a bias decomposition and design-based metrics that characterize bias due to estimand mismatch (i.e., deviation from the population of interest) and statistical bias, allowing one to characterize how the choice of estimand impacts performance along these facets. Our estimand selection procedure identifies a sequence of estimands whose corresponding estimators tend to have reduced MSE with respect the target estimand and a clear interpretation in respect to the bias-variance tradeoff. In addition, our selection procedure is flexible and allows the analyst to incorporate their domain-specific preferences.

While we present methods and results with respect to the ATE as the estimand of scientific interest, these methods can be applied to any other estimand such as the ATT or when transporting effects to a new population. In addition, our methods could be extended to regression augmented estimators, though further work is needed to assess how well our proposed metric (Section 3.2) characterizes statistical bias in these cases. Furthermore, while we explore the set of estimands in Equation (3), any potential set of estimands defined by weighted populations could be explored. Identifying a different set of potential estimands may be important when transporting effects as the there is no guarantee that a new population is similar to the weighted populations defined by Equation (3).

We acknowledge that using our proposed procedure to identify an estimand could influence downstream inference. However, the majority of our procedure is design-based which helps protect against possible impacts on inference when using an estimand selected through this procedure. In fact, the procedure could be made entirely design-based. For example, one could assume a structure for the residual variance (e.g., homoscedasticity) such that some identifiable $h^*(\mathbf{x})$, that is a function of only covariates, achieves minimum asymptotic variance. Then, instead of selecting the $h_{c,d}(\mathbf{x})$ with the smallest estimated standard error for each estimand mismatch contour level, we could select the $h_{c,d}(\mathbf{x})$ that minimizes some distance to $h^*(\mathbf{x})$ (e.g., Euclidean distance on the $c, d \in [0, 1] \times [0, 1]$ space). Further, Yang and Ding (2018) provide methods for incorporating uncertainty from both the design and analysis stage in the inferential procedure when using continuous weights that could be used.

Funding

The first author was supported by the National Science Foundation Graduate Research Fellowship Program under Grant No. 2237827.

Code and Data

The Git repository https://github.com/m-barnard/estimand_selection contains data and code to replicate the analyses and to implement the estimand selection procedure on a new dataset.

References

- Busso, M., DiNardo, J., and McCrary, J. (2014). New Evidence on the Finite Sample Properties of Propensity Score Reweighting and Matching Estimators. The Review of Economics and Statistics **96**, 885–897.
- Chattopadhyay, A., Hase, C. H., and Zubizarreta, J. R. (2020). Balancing vs modeling approaches to weighting in practice. Statistics in Medicine **39**, 3227–3254.
- Connors, A. F., Speroff, T., Dawson, N. V., Thomas, C., Harrell, F. E., Wagner, D. et al. (1996). The effectiveness of right heart catheterization in the initial care of critically ill patients. SUPPORT Investigators. JAMA **276**, 889–897.
- Crump, R. K., Hotz, V. J., Imbens, G. W., and Mitnik, O. A. (2009). Dealing with limited overlap in estimation of average treatment effects. Biometrika **96**, 187–199.
- de los Angeles Resa, M., and Zubizarreta, J. R. (2016). Evaluation of subset matching methods and forms of covariate balance. Statistics in Medicine **35**, 4961–4979.
- Faigle, R., Ziai, W. C., Urrutia, V. C., Cooper, L. A., and Gottesman, R. F. (2017). Racial differences in palliative care use after stroke in majority-white, minority-serving, and racially integrated US hospitals. Critical care medicine **45**, 2046–2054.
- Fogarty, C. B., Mikkelsen, M. E., Gaieski, D. F., and Small, D. S. (2016). Discrete Optimization for Interpretable Study Populations and Randomization Inference in an Observational Study of Severe Sepsis Mortality. Journal of the American Statistical Association .

- Hahn, J. (1998). On the Role of the Propensity Score in Efficient Semiparametric Estimation of Average Treatment Effects. Econometrica **66**, 315–332.
- Hainmueller, J. (2012). Entropy Balancing for Causal Effects: A Multivariate Reweighting Method to Produce Balanced Samples in Observational Studies. Political Analysis **20**, 25–46.
- Hernan, M. A., and Robins, J. M. (2024). Causal Inference: What If. CRC Press.
- Hirano, K., and Imbens, G. W. (2001). Estimation of Causal Effects using Propensity Score Weighting: An Application to Data on Right Heart Catheterization. Health Services and Outcomes Research Methodology **2**, 259–278.
- Hirano, K., Imbens, G. W., and Ridder, G. (2003). Efficient Estimation of Average Treatment Effects Using the Estimated Propensity Score. Econometrica **71**, 1161–1189.
- Hong, H., Leung, M. P., and Li, J. (2020). Inference on finite-population treatment effects under limited overlap. The Econometrics Journal **23**, 32–47.
- Huling, J. D., and Mak, S. (2024). Energy balancing of covariate distributions. Journal of Causal Inference **12**,.
- Imbens, G. W. (2004). Nonparametric Estimation of Average Treatment Effects Under Exogeneity: A Review. The Review of Economics and Statistics **86**, 4–29.
- Li, F., Morgan, K. L., and Zaslavsky, A. M. (2018). Balancing Covariates via Propensity Score Weighting. Journal of the American Statistical Association .
- Li, F., Thomas, L. E., and Li, F. (2019). Addressing Extreme Propensity Scores via the Overlap Weights. American Journal of Epidemiology **188**, 250–257.
- Li, L., and Greene, T. (2013). A weighting analogue to pair matching in propensity score analysis. The International Journal of Biostatistics **9**, 215–234.
- Mao, H., Li, L., and Greene, T. (2019). Propensity score weighting analysis and treatment effect discovery. Statistical Methods in Medical Research **28**, 2439–2454.
- Neyman, J. (1990). On the Application of Probability Theory to Agricultural Experiments. Essay on Principles. Section 9. Statistical Science **5**, 465–472.
- Raeisi-Giglou, P., Jabri, A., Shahreri, Z., Sallam, S., Alhuneafat, L., Al-abdouh, A. et al. (2022). Disparities in the Prescription of Statins in the Primary Care Setting: A Retrospective Observational Study. Current Problems in Cardiology **47**, 101329.
- Robins, J. M., Hernán, M. A., and Brumback, B. (2000). Marginal structural models and causal inference in epidemiology. Epidemiology (Cambridge, Mass.) **11**, 550–560.
- Rosenbaum, P. R. (2012). Optimal Matching of an Optimally Chosen Subset in Observational Studies. Journal of Computational and Graphical Statistics **21**, 57–71.

- Rosenbaum, P. R., and Rubin, D. B. (1983a). Assessing Sensitivity to an Unobserved Binary Covariate in an Observational Study with Binary Outcome. Journal of the Royal Statistical Society. Series B (Methodological) **45**, 212–218.
- Rosenbaum, P. R., and Rubin, D. B. (1983b). The central role of the propensity score in observational studies for causal effects. Biometrika **70**, 41–55.
- Rubin, D. B. (1974). Estimating causal effects of treatments in randomized and nonrandomized studies. Journal of Educational Psychology **66**, 688–701.
- Rubin, D. B. (1978). Bayesian Inference for Causal Effects: The Role of Randomization. The Annals of Statistics **6**, 34–58.
- Tchikrizov, V., Ladner, M. E., Caples, F. V., Morris, M., Spillers, H., Jordan, C. D. et al. (2023). Health disparities in the treatment of bipolar disorder. Personalized Medicine in Psychiatry **37-38**, 100101.
- Traskin, M., and Small, D. S. (2011). Defining the Study Population for an Observational Study to Ensure Sufficient Overlap: A Tree Approach. Statistics in Biosciences **3**, 94–118.
- Visconti, G., and Zubizarreta, J. (2018). Handling Limited Overlap in Observational Studies with Cardinality Matching. Observational Studies **4**, 217–249.
- Wang, Y., and Zubizarreta, J. R. (2020). Minimal dispersion approximately balancing weights: asymptotic properties and practical considerations. Biometrika **107**, 93–105.
- Yang, S., and Ding, P. (2018). Asymptotic inference of causal effects with observational studies trimmed by the estimated propensity scores. Biometrika **105**, 487–493.
- Zubizarreta, J. R. (2015). Stable Weights that Balance Covariates for Estimation With Incomplete Outcome Data. Journal of the American Statistical Association **110**, 910–922.

Supplementary Materials

Appendix A

Proof. By Theorem 2 of Li et al. (2018), for a sample $\mathbf{X} = \{\mathbf{x}_1, \dots, \mathbf{x}_n\}$, as $n \rightarrow \infty$,

$$nE_{\mathbf{x}}\{\text{Var}(\hat{t}_h|\mathbf{X})\} \rightarrow \frac{1}{C_h^2} \int f(\mathbf{x})h(\mathbf{x})^2[v_1(\mathbf{x})/e(\mathbf{x}) + v_0(\mathbf{x})/\{1 - e(\mathbf{x})\}]d\mathbf{x}.$$

where $v_z(\mathbf{x}) = \text{Var}\{Y(z)|\mathbf{X} = \mathbf{x}\}$ and $C_h = \int h(\mathbf{x})f(\mathbf{x})d\mathbf{x}$. Let $v \in \mathbb{R}^+$ and functions $h^*(\mathbf{x}), k_0(\mathbf{x}), k_1(\mathbf{x}) > 0$ for all \mathbf{x} . Now, consider $v_0(\mathbf{x}) = v \frac{k_0(\mathbf{x})\{1-e(\mathbf{x})\}}{h^*(\mathbf{x})\{k_0(\mathbf{x})+k_1(\mathbf{x})\}}$ and $v_1(\mathbf{x}) = v \frac{k_1(\mathbf{x})e(\mathbf{x})}{h^*(\mathbf{x})\{k_0(\mathbf{x})+k_1(\mathbf{x})\}}$ such that as $n \rightarrow \infty$,

$$nE_{\mathbf{x}}\{\text{Var}(\hat{t}_h|\mathbf{X})\} \rightarrow \frac{v}{C_h^2} \int f(\mathbf{x})h(\mathbf{x})^2 \frac{k_0(\mathbf{x}) + k_1(\mathbf{x})}{h^*(\mathbf{x})\{k_0(\mathbf{x}) + k_1(\mathbf{x})\}} d\mathbf{x}, \quad (8)$$

$$\rightarrow \frac{v}{C_h^2} \int \frac{f(\mathbf{x})h(\mathbf{x})^2}{h^*(\mathbf{x})} d\mathbf{x}. \quad (9)$$

For clarity in notation, $E[\cdot]$ indicates $\int \cdot f(\mathbf{x})d\mathbf{x}$. Using the same argument as the proof of Corollary 1 in Li et al. (2018), by the Cauchy-Schwartz inequality

$$\begin{aligned} E\{h(\mathbf{x})\}^2 &= \left[E \left\{ \frac{h(\mathbf{x})}{\sqrt{h^*(\mathbf{x})}} \sqrt{h^*(\mathbf{x})} \right\} \right]^2, \\ &\leq E \left\{ \frac{h(\mathbf{x})^2}{h^*(\mathbf{x})} \right\} E\{h^*(\mathbf{x})\}, \end{aligned}$$

where equality holds when $h(\mathbf{x}) \propto h^*(\mathbf{x})$. Applying this result to the right-hand side of (9), we have that as $n \rightarrow \infty$

$$n \min_h (E_{\mathbf{x}}\{\text{Var}(\hat{t}_h|\mathbf{X})\}) \rightarrow \frac{v}{C_h^2} \int f(\mathbf{x})h^*(\mathbf{x})d\mathbf{x},$$

and $h(\mathbf{x}) \propto h^*(\mathbf{x})$ gives the smallest asymptotic variance for $\hat{\tau}_h$ among all h . □

Supplementary Tables and Figures

Table 1: Common causal estimands and their corresponding $h(\mathbf{x})$, balancing weights (Li et al., 2018), and population.

Estimand	$h(\mathbf{x})$	$w_0(\mathbf{x}), w_1(\mathbf{x})$	Target Population
ATE	1	$1/\{1 - e(\mathbf{x})\}, 1/e(\mathbf{x})$	Combined
ATT	$e(\mathbf{x})$	$e(\mathbf{x})/\{1 - e(\mathbf{x})\}, 1$	Treated
ATC	$1 - e(\mathbf{x})$	$1, e(\mathbf{x})/\{1 - e(\mathbf{x})\}$	Control
ATO	$e(\mathbf{x})\{1 - e(\mathbf{x})\}$	$e(\mathbf{x}), 1 - e(\mathbf{x})$	Overlap

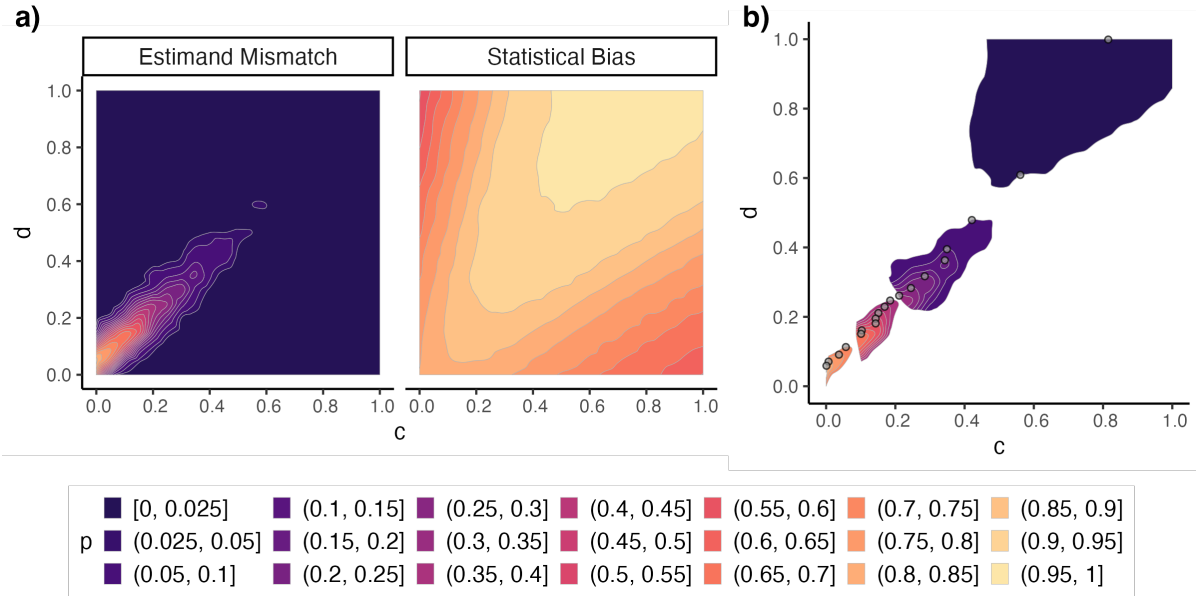


Figure 1: Subfigure a) shows the contours of the p -values corresponding to estimand mismatch and statistical bias. Data is interpolated using cubic splines in order to smooth contours. Subfigure b) shows the intersection of each estimand mismatch p -value contour with the largest statistical bias p -value contour level (color indicates the estimand mismatch p -value contour level). The points in subfigure b) show the selected estimands for each estimand mismatch p -value contour.

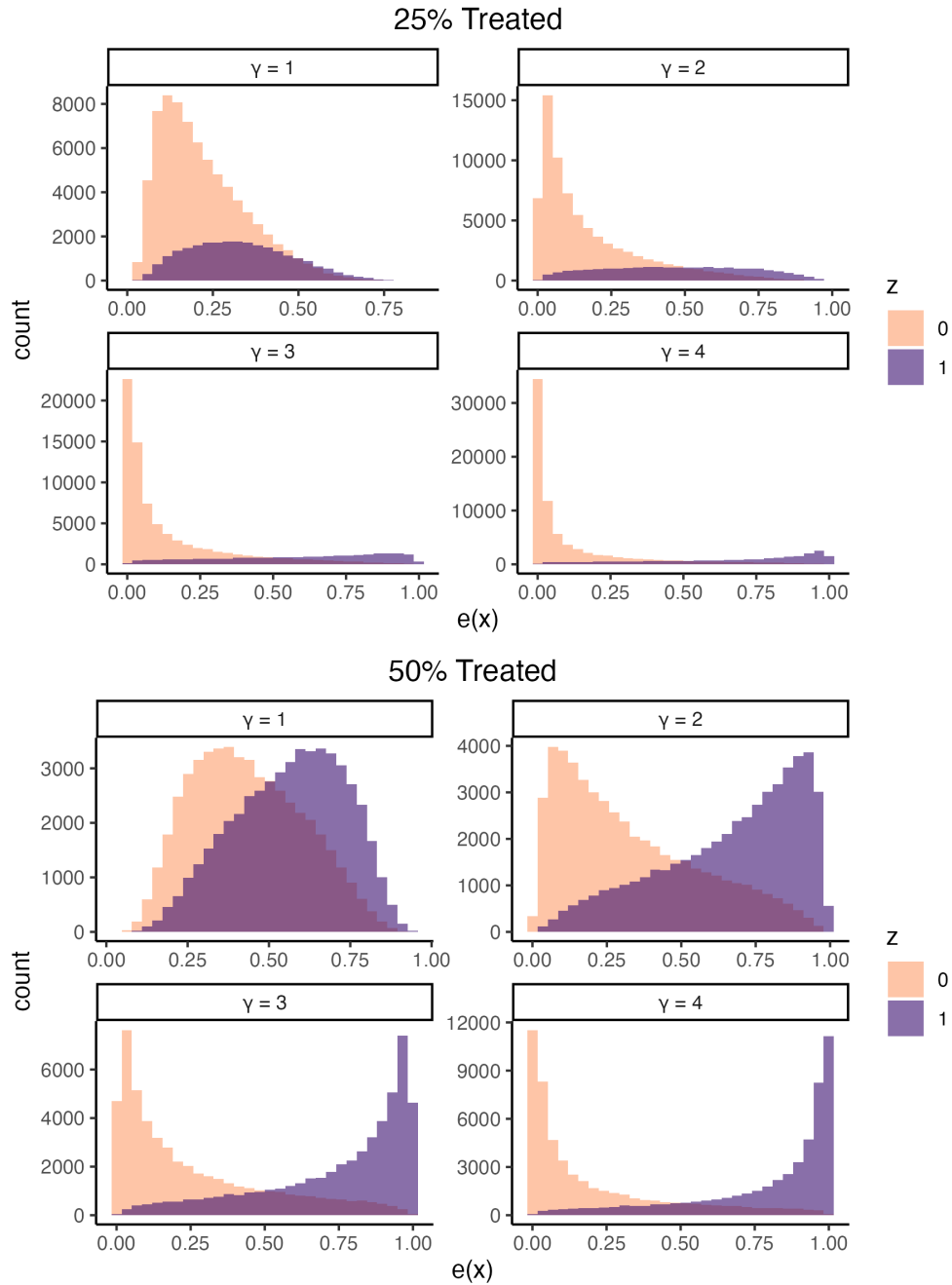


Figure 2: Propensity score overlap for all simulation scenarios. The top and bottom four panels show overlap for simulated data with 25% and 50% of individuals treated, respectively. Note that γ indicates the level of propensity score overlap where $\gamma = 1$ is high overlap and $\gamma = 4$ is low overlap.

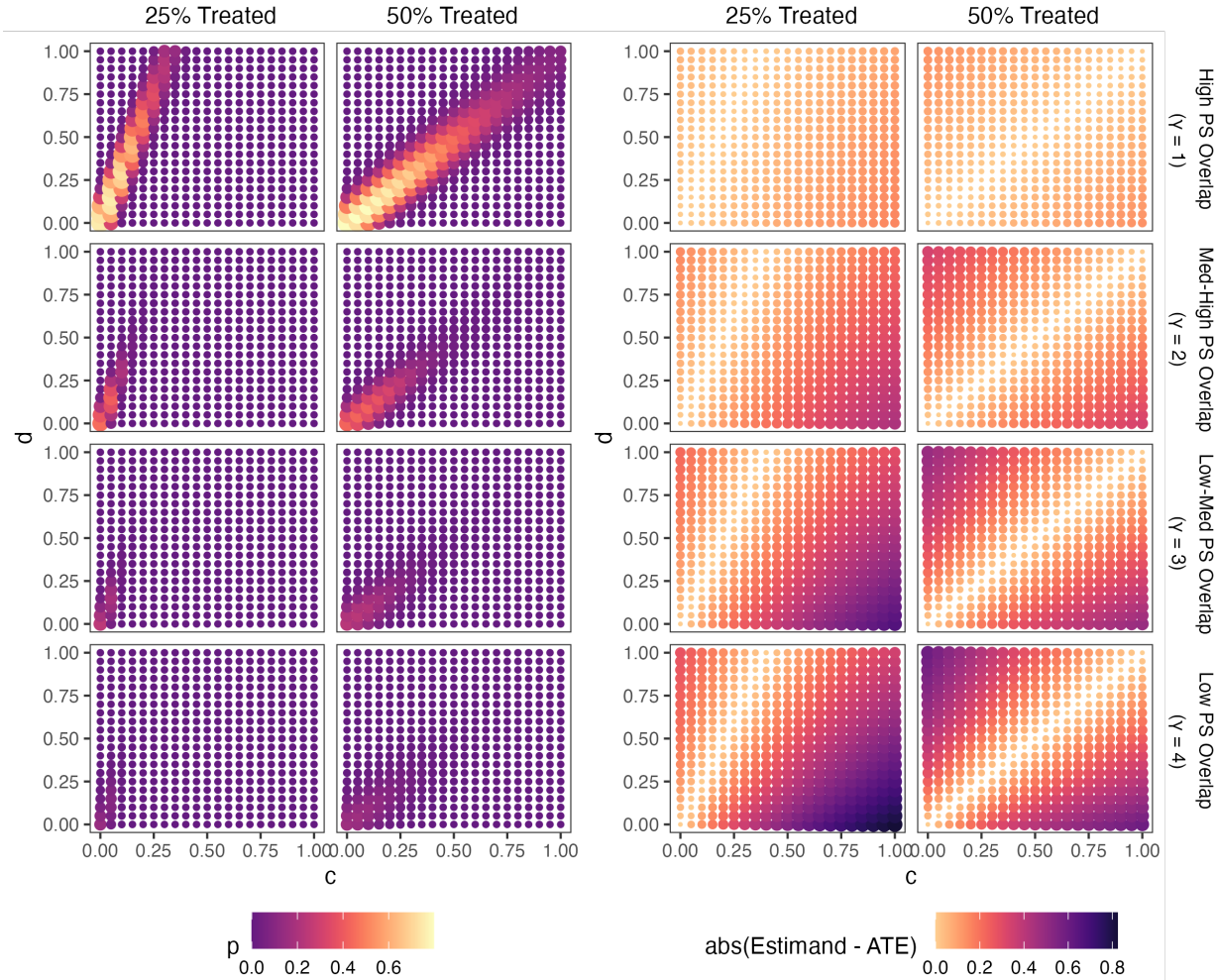


Figure 3: The left panel presents the average of the minimum of the two estimand mismatch related p -values, calculated as described in Section 3.1, for each estimand. The right panel presents the absolute difference between the true estimands and the true ATE (i.e., the absolute estimand mismatch) under the medium Δ heterogeneity scenario when simulating the treatment effect as a linear function of the propensity score. Columns distinguish the 25% and 50% treated scenarios while rows distinguish the different propensity score overlap scenarios.

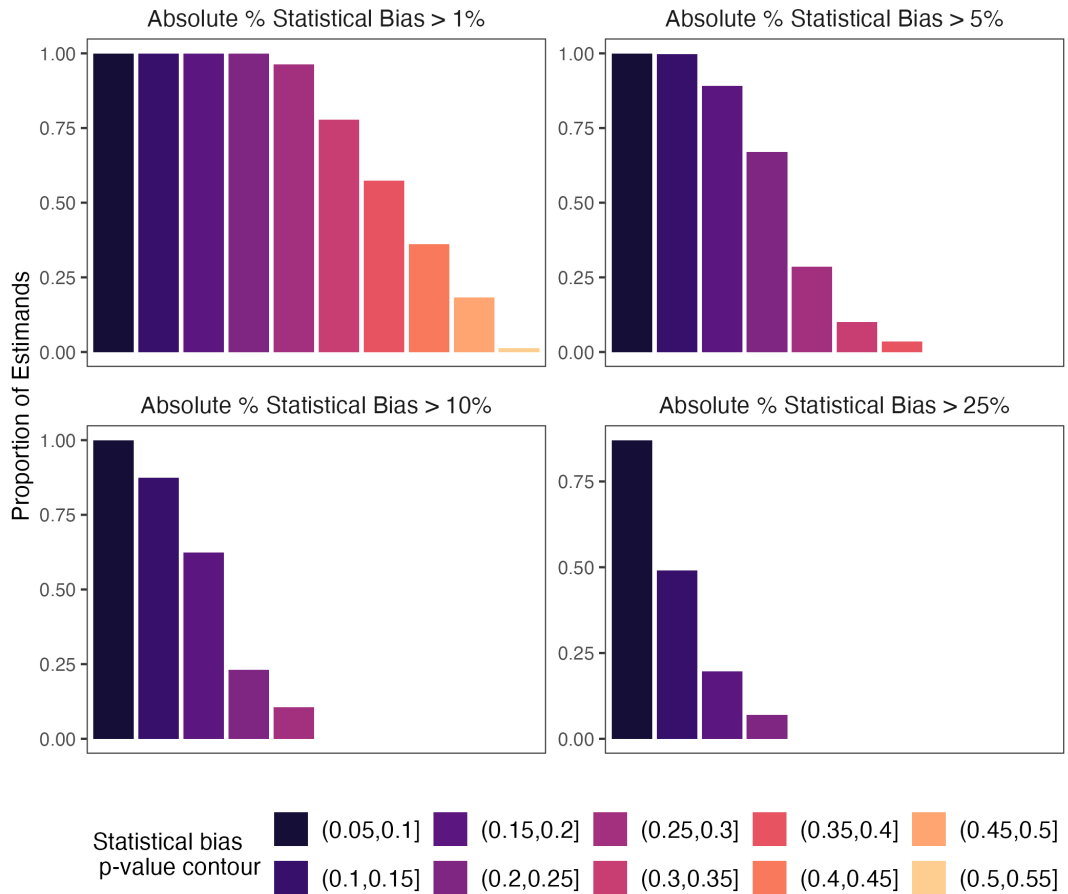


Figure 4: Proportion of estimands within each statistical bias associated p -value contour with absolute percent bias greater than 1%, 5%, 10%, and 25%.

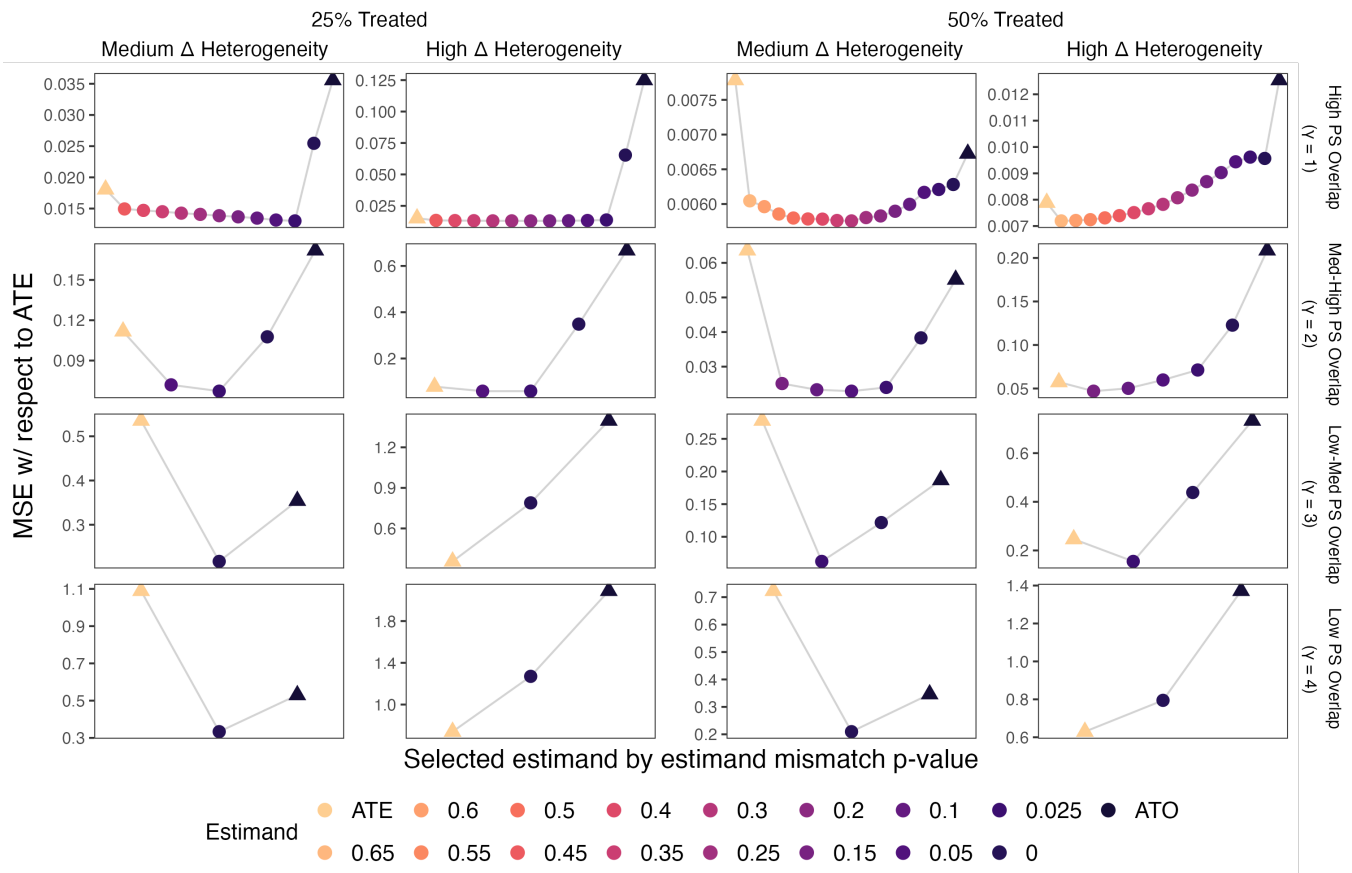


Figure 5: Mean squared error (MSE) with respect to the true ATE for the estimators for the ATE, the estimands selected with our procedure, and the ATO. Each of the 16 subplots corresponds to a single simulation scenario as labeled by the top and right axes. Estimands are labeled by the lower bound of their corresponding estimand mismatch p -value contour. Estimands selected (i.e., estimand mismatch p -value contours present) in at least 900 of the simulated datasets are shown.

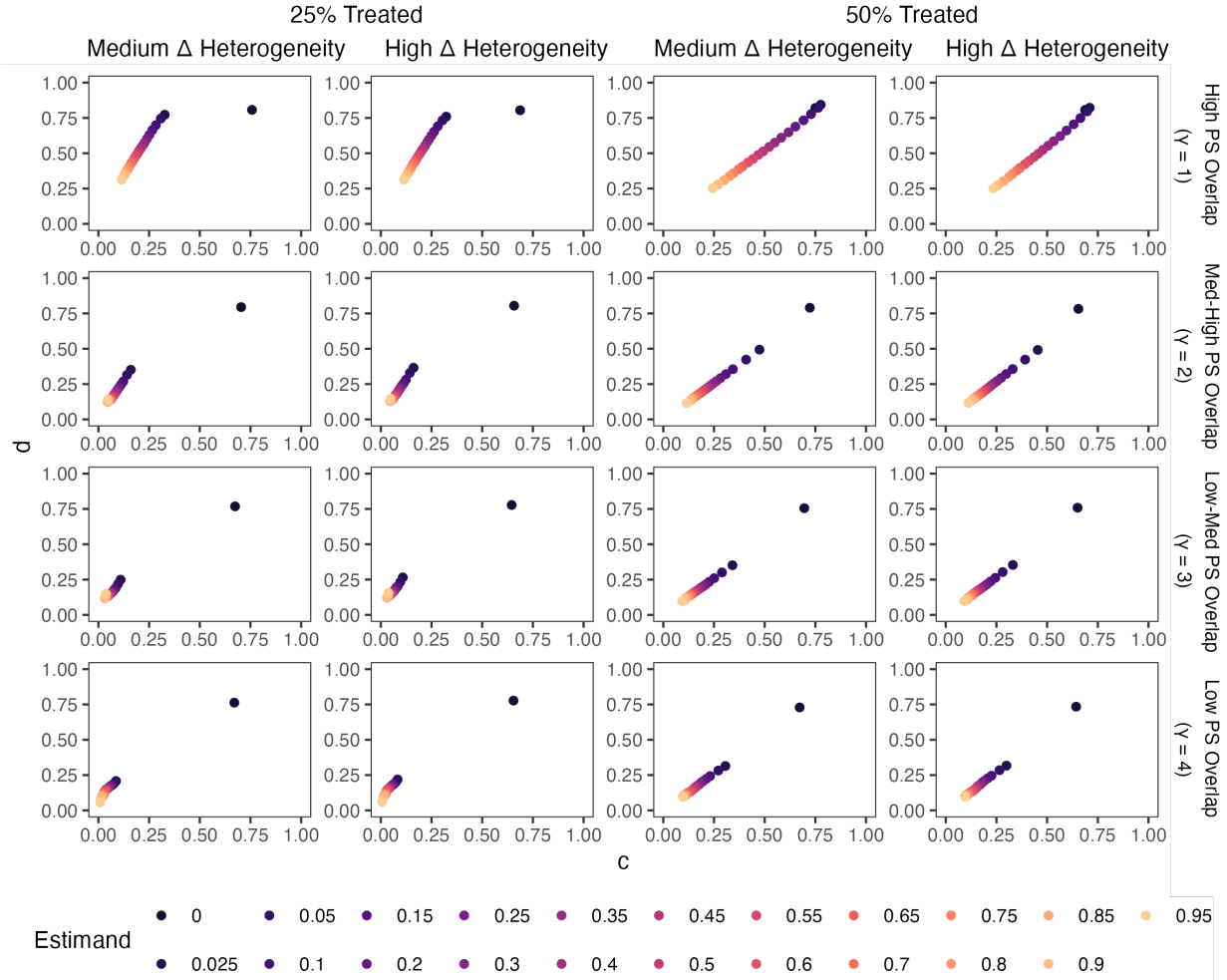


Figure 6: Average of the selected estimands (i.e., average of c and d) for each estimand mismatch p -value contour across all possible simulated datasets. Each of the 16 subplots corresponds to a single simulation scenario as labeled by the top and right axes. Estimands are labeled by the lower bound of their corresponding estimand mismatch p -value contour.

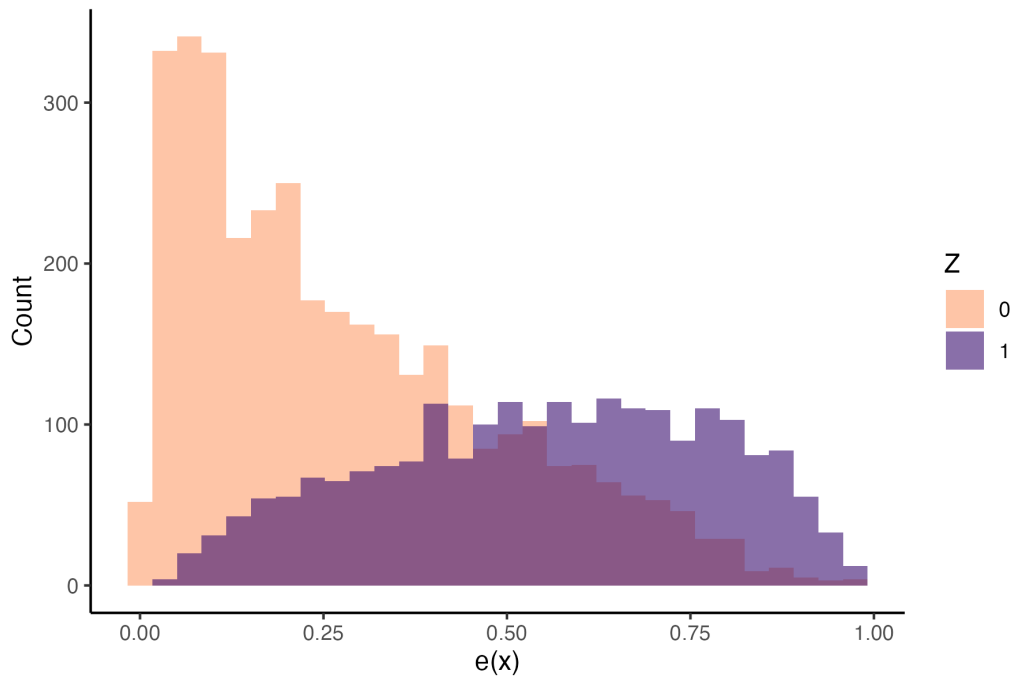


Figure 7: Estimated propensity score distributions of treated and control groups for the right heart catheterization study (Connors et al., 1996).

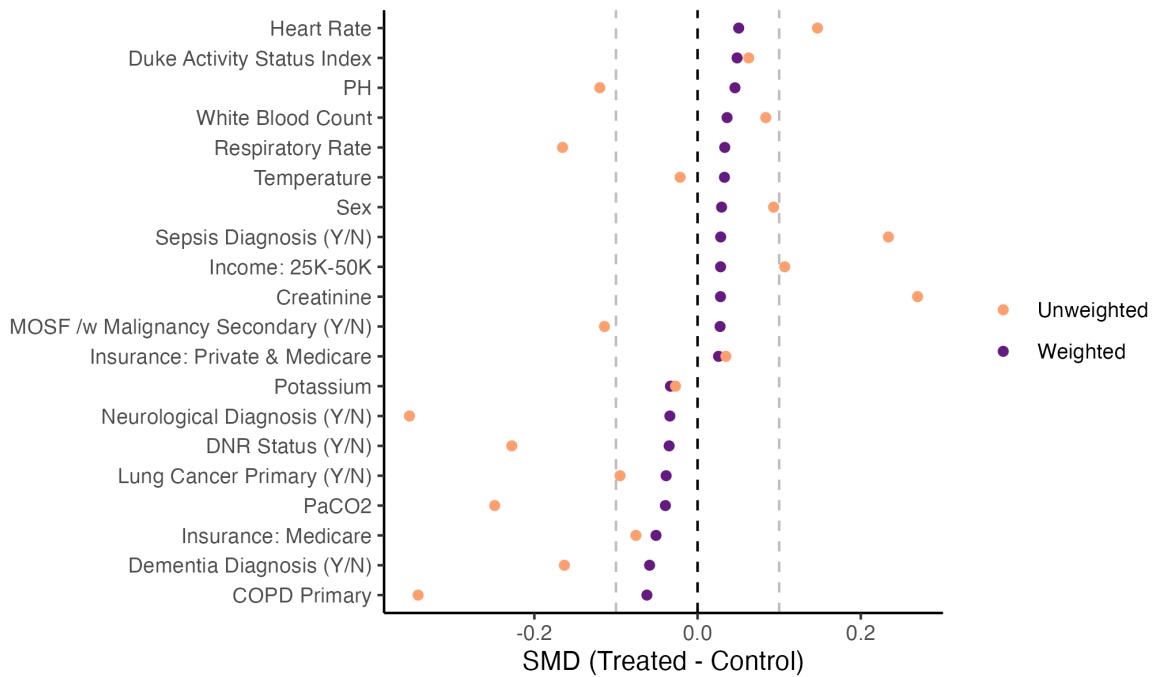


Figure 8: Standardized mean difference (SMD) of the twenty most imbalanced covariates after IPW weighting for the right heart catheterization study (Connors et al., 1996).